A topological study of bonding in aquo and bis-triazinyl-pyridine complexes of trivalent lanthanides and actinides: does covalency imply stability?

Izaak Fryer-Kanssen[1], Jonathan Austin[2] and Andrew Kerridge[1]*

[1]Department of Chemistry, Lancaster University, Bailrigg, Lancaster, LA1 4YB, UK

2 National Nuclear Laboratory, Chadwick House, Birchwood Park, Warrington, WA3 6AE, UK

*a.kerridge@lancaster.ac.uk

Abstract

The geometrical and electronic structures of $Ln[(H_2O)_9]^{3+}$ and $[Ln(BTP)_3]^{3+}$, where Ln = Ce – Lu, have been evaluated at the density functional level of theory using three related exchange-correlation (*xc*-) functionals. The BHLYP *xc*-functional was found to be most accurate and this, along with the B3LYP functional, was used as the basis for topological studies of the electron density via the Quantum Theory of Atoms in Molecules (QTAIM). This analysis revealed that, for both sets of complexes, bonding was almost identical across the Ln series and was dominated by ionic interactions. Geometrical and electronic structures of actinide (An = Am, Cm) analogues were evaluated and $[An(H_2O)_9]^{3+} + [Ln(BTP)_3]^{3+} \rightarrow [Ln(H_2O)_9]^{3+} + [An(BTP)_3]^{3+}$ exchange reaction energies were evaluated, revealing Eu $\leftrightarrow$ Am and Gd $\leftrightarrow$ Cm reactions to favour the actinide species. Detailed QTAIM analysis of Eu, Gd, Am and Cm complexes revealed increased covalent character in M – O and M – N bonds when M = An, with this increase being more pronounced in the BTP complexes. This therefore implies a small electronic contribution to An – N bond stability and the experimentally observed selectivity of the BTP ligand for Am and Cm over lanthanides.

Introduction

The technological applications of the lanthanides are numerous and varied, however lanthanides can also manifest themselves as unwanted components of materials. An example material is spent nuclear fuel: as an example, the distribution of ^{235}U fission products exhibits two peaks in yield, one of which is centred at a relative atomic mass $A_r \simeq 138$. The presence of lanthanides in spent nuclear fuel increases the difficulty of both its disposal and its potential recyclability. In the former, the relatively short lanthanide (Ln) half-lives, when compared to those of the actinides (An), means that greater volumes than necessary currently need to be disposed of in long-term storage facilities, whilst in the latter a hurdle arises due to the strong neutron absorption cross sections of lanthanides. These issues can be effectively surmounted by the separation of lanthanides from actinides in the spent fuel. However, this becomes technically challenging when considering the later actinides such as americium and curium, whose chemistry strongly resembles that of the trivalent lanthanides. Significant progress has been made in developing solvent extraction methodologies for the separation of trivalent lanthanides from the so-called minor actinides (MAs, typically considered to comprise Np, Am and Cm)[1–3].

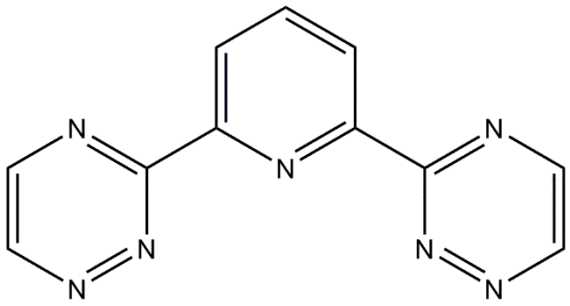

Figure 1. The bis-triazinyl-pyridine (BTP) ligand considered in this study

Several nitrogen donor ligands, such as BTP (2,6-bis(1,2,4-triazin-3-yl)pyridine, Figure 1), BTBP (6,6'-bis(1,2,4-triazin-3-yl)-2,2'-bipyridine) and BTPhen (2,9-bis(1,2,4-triazin-3-yl)-1,10-phenanthroline) have been developed and investigated for Ln(III)/An(III) separation, showing strong

selectivity for the latter[4,5]. Whilst BTBP and BTPhen offer improvements, namely back-extraction and increased actinide selectivity, BTP was the first N-donor extraction ligand to exhibit excellent selectivity ($SF_{Am/Eu}$ up to 150) under highly acidic conditions (1 M HNO_3)[4–6]. However, despite almost two decades of research since the solvent extraction ability of BTP was reported by Kolarik *et al*[6,7] in 1999, the exact origin of this selectivity is still unclear.

Quantum-chemical calculations have been used alongside analytical methods to investigate the differences in structure between selected Ln(III) and An(III) complexes. A combined effort of electrospray mass spectroscopy[8,9], time-resolved laser-induced fluorescence spectroscopy (TRLFS)[10–16], X-ray photoelectron spectroscopy (XPS) and extended X-ray absorption fine structure spectroscopy (EXAFS)[15–21] with complementary density functional theory (DFT) studies[16,18] have probed the structure of $[Ln/An(BTP)_n]^{3+}$ (n = 1-3), with a general focus on the complexes of Ln = Eu, Gd and An = U–Cm due to their relevance to the separation process. For the lanthanides, a trend of decreasing metal-ligand bond length with decreasing Ln(III) ionic radius was observed spectroscopically[15–21]. This was in contrast to the bond lengths of the actinide complexes, which were observed to be largely independent of An(III) ionic radius, and this structural difference was reproduced when investigated using quantum chemical methods provided that the f-electrons were treated explicitly, i.e. not considered core-like and replaced by a pseudopotential[15,18,22,23].

As well as being a complementary method, there are also many primarily computational studies of Ln(III) and An(III) complexes in the literature, both for ligands such as BTP, BTBP and BTPhen and other nitrogen donor ligands[24–37]. Key to several of these studies are the differences in energies of the Ln(III) and An(III) complexes and, despite the large separation factors exhibited by these ligands, these energetic differences amount to only hundredths to tenths of an eV.[24–26,33] For instance, Lan *et al.* report that for the reaction $M(NO_3)_3(H_2O)_4 + L \rightarrow M(L)(NO_3)_3 + 4H_2O$, (L = BTBPs) the formation of $M(L)(NO_3)_3$ is favoured energetically when M = Am compared to M = Eu by a 0.13 eV in the DFT-calculated Gibbs free energy for L = BTBP and 0.07 eV for L = $CyMe_4$-BTBP[25], obtained

using the B3LYP exchange-correlation (*xc*-)functional. For BTP, Trumm *et al.* report the formation of the Cm complex to be 2.3 kcal/mol (~0.1 eV) more favourable than Gd in the gas-phase, calculated at the MP2 level on DFT structures optimised using the BHLYP *xc*-functional. Additionally, lanthanide (III) hydration has been studied both experimentally and with quantum-chemical methods, finding a 9-coordinate $[Ln(H_2O)_9]^{3+}$ structure with tricapped trigonal prism geometry for the early and mid-series lanthanides that gradually becomes 8-coordinate, albeit as a dynamic equilibrium[38]. The same trends in coordination were observed for actinide (III) hydration[38].

One of the underlying mechanisms responsible for the selective binding of MAs by soft-donor ligands is believed to be the greater availability of actinide 5f-orbitals in comparison to the core-like 4f-orbitals of their lanthanide analogues. If this is the case, the availability of the 5f-manifold should manifest itself in enhanced covalency in MA-ligand bonding. The complex electronic structure of f-element compounds however presents significant challenges in the assessment and quantification of covalent contributions to bonding, and recently attention has turned towards density-based measures of analysis. Foremost amongst these approaches is Bader's Quantum Theory of Atoms in Molecules (QTAIM)[39], which provides a robust and rigorous framework for the partitioning of a molecular system into a set of contiguous, space-filling volumes, or atomic basins, each of which satisfies the criteria of a proper open quantum system. The QTAIM approach allows for the unambiguous characterisation of bonding in terms of both topological and integrated properties of the experimentally observable electron density and has been successfully applied in the characterisation of bonding of actinides in a variety of oxidation states and coordination environments[40–46]. More recently, evidence has emerged for correlations between QTAIM measures of covalent bonding character and bond stability[47–50]. QTAIM studies of lanthanide complexes are less common. There are a small number of Ce(IV) studies[51–54], and a comparable number focussing on trivalent lanthanides[32,53,55,56], but there is no systematic study across the lanthanide series. The lanthanides are typically considered as being essentially ionic in their interactions, and so would be expected to exhibit similar QTAIM-derived characteristics, however recent studies have revealed unexpected levels of covalency in Ce(IV) compounds[53,54,57] and even evidence of covalency in Ln(III)

compounds[58,59]. It is therefore important to verify the assumption of ionic lanthanide bonding character within the QTAIM framework if it is to have general applicability in the development of our understanding of the Ln(III)/An(III) separation process. In this contribution we present the first systematic study of the topological and integrated electronic properties of aquo and BTP complexes of the lanthanides (Ce-Lu) and compare them to complexes of two technologically relevant actinides (Am and Cm) in order to investigate the relationship between bond covalency and complex stability.

Computational Details

All calculations were performed using version 6.6 of the TURBOMOLE quantum chemistry code[60] using scalar-relativistic DFT. Several *xc*-functionals were considered in order to identify which was most suitable for these simulations: BLYP[61,62], a functional based on the generalised gradient approximation (GGA), and two hybrid GGA-functionals, B3LYP[63,64] and BHLYP[65], which incorporate 20% and 50%, respectively, of exact exchange into the exchange component of the functional. All optimisations were performed using def-SVP (Ln, An) and def2-SVP (H, C, N, O) basis sets of polarised double-ζ quality,[66] referred to from here on as def(2)-SVP. Actinide and lanthanide core electrons were replaced with the small-core pseudopotentials of Dolg and coworkers[67–69]. Subsequent single point energy calculations were performed using the def(2)-TZVP basis sets of polarised triple-ζ quality.[66] Geometry optimisations were performed using default convergence criteria in both the presence and absence of a water-like continuum solvent defined using the COSMO model[70] with the default radii r_O = 1.72 Å, r_C = 2.00 Å, r_N = 1.83 Å, r_H = 1.30 Å, r_{Ln} = 2.22 Å, r_{An} = 2.22 Å. Local energetic minima were identified via numerical frequency analysis. For a subset of systems, all-electron single-point energy calculations were performed. The calculations used SARC basis sets of polarised triple-ζ quality for the heavy elements[71,72]. In these all-electron calculations, scalar relativistic effects were incorporated by using the 2nd order Douglas-Kroll-Hess

(DKH) Hamiltonian[73,74]. Topological and integrated properties of the electron density were performed using the AIMAll[75] (Version 14) and Multiwfn[76] (Version 3.3) codes.

Results and Discussion

Structural Characterisation

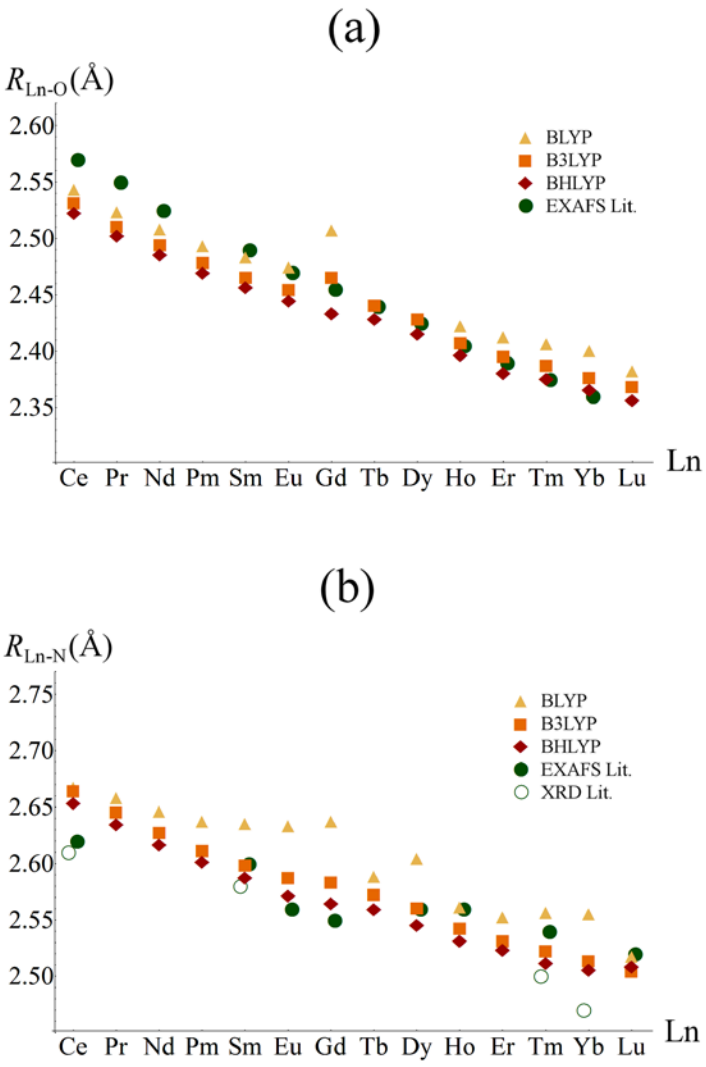

Figure 2. (a): Average Ln-O bond lengths of $[Ln(H_2O)_9]^{3+}$ (Ln = Ce – Lu) calculated with DFT (present work) and obtained experimentally via EXAFS[77]; (b): Average Ln-N bond lengths of $[Ln(BTP)_3]^{3+}$ calculated with DFT (present work) and obtained experimentally via EXAFS and XRD[15–21]. Literature data has been offset by ± 0.1 on the x-axis for readability.

Figure 2a compares Ln-O bond lengths of $[Ln(H_2O)_9]^{3+}$ (Ln = Ce – Lu) obtained experimentally via EXAFS[77] to our DFT-optimised values, obtained in the presence of a continuum solvent. From these data, a clear trend can be identified. For early lanthanides, M-O bond lengths are underestimated, whereas agreement improves significantly as the series is traversed, with hybrid functionals giving best agreement. The BHLYP functional typically gives Ln-O bond lengths ~ 0.02 - 0.03 Å shorter than those obtained with BLYP, although this difference is significantly more pronounced around the middle of the series (Gd – Dy), where BLYP appears to severely overestimate and, in the case of Tb, failed, despite repeated attempts, to return an optimised structure. B3LYP bond lengths are much closer to BHLYP values, typically just 0.01Å longer, although this difference is again more pronounced when Ln = Gd. Gas phase bond lengths are typically ~ 0.05 Å longer than those obtained in the presence of the continuum solvent and are consistently greater than experimental values, demonstrating the improved structural description obtained using a continuum solvent model. Additionally, when compared to calculated BP86 gas phase bond lengths reported in literature[78], B3LYP and BH-LYP gas phase bond lengths are typically ~ 0.01 Å and ~ 0.03 Å shorter respectively, while BLYP gas phase bond lengths are typically identical.

When considering $[Ln(BTP)_3]^{3+}$ EXAFS and XPS data[15–21], the trend in Ln-N bond lengths is less clear than in the aquo complexes. However, for the lighter lanthanides, our simulations show that all three *xc*-functionals overestimate these bond lengths, with agreement improving as the series is traversed. Again, BLYP significantly overestimates bond lengths for Eu – Dy, as well as for some elements towards the end of the series. BHLYP and B3LYP give similar bond lengths, with the latter again ~ 0.01 Å longer than the former. For Gd, BHLYP, in combination with a continuum solvent model, gives an average bond length ~ 0.01 Å shorter than the gas phase BHLYP value reported by Trumm *et al*[24]. For Eu, the BHLYP value of 2.572 Å is closer to the literature RI-MP2 value[16] of 2.556 Å than gas phase literature values obtained with BLYP, B3LYP and BHLYP (2.654 Å, 2.633 Å and 2.614 Å respectively[16]).

Table 1. Comparison of theoretical and calculated expectation values of $\hat{S}^2$ obtained with different *xc*-functionals and the def-SVP basis set. Values are omitted when electronic structure failed to converge.

Ln	*S*	*S*(*S*+1)	$\langle\hat{S}^2\rangle$					
			$[Ln(H_2O)_9]^{3+}$			$[Ln(BTP)_3]^{3+}$		
			BLYP	B3LYP	BHLYP	BLYP	B3LYP	BHLYP
Ce	1/2	0.75	0.75	0.75	0.75	0.75	0.75	0.75
Pr	1	2.00	2.00	2.00	2.00	2.00	2.00	2.00
Nd	3/2	3.75	3.75	3.75	3.75	3.76	3.75	3.75
Pm	2	6.00	6.01	6.00	6.00	6.03	6.01	6.00
Sm	5/2	8.75	8.78	8.76	8.75	8.87	8.76	8.75
Eu	3	12.00	12.05	12.01	12.01	12.21	12.01	12.01
Gd	7/2	15.75	16.08	15.96	15.76	16.12	15.87	15.76
Tb	3	12.00	-	12.60	12.60	13.03	12.56	12.56
Dy	5/2	8.75	-	9.27	9.25	9.48	9.23	9.20
Ho	2	6.00	6.00	6.00	6.00	6.00	6.00	6.00
Er	3/2	3.75	3.75	3.75	3.75	3.75	3.75	3.75
Tm	1	2.00	2.00	2.00	2.00	2.00	2.00	2.00
Yb	1/2	0.75	0.75	0.75	0.75	0.75	0.75	0.75
Lu	0	0	0	0	0	0	0	0

To further investigate the poor quality of BLYP-calculated structures as seen in Figure 2, we considered the expectation values of $\hat{S}^2$, which are reported in Table 1. When compared to theoretical expectation values, $\langle\hat{S}^2\rangle = S(S+1)$, it can be seen that, in the BTP complexes, BLYP-calculated values are significantly too large between Eu and Dy. This is also the case in the Gd aquo complex, and is indicative of significant spin-contamination. The inclusion of exact exchange significantly

reduces spin-contamination, although this remains pronounced for Tb and Dy complexes, where contamination comprises approximately 5% of the total value.

The results presented in Table 1, taken in the context of the data presented in Figure 2, indicate that the origin of the poor performance of the BLYP-functional in simulating the structural properties of the lanthanide complexes under consideration here is in the description of the electronic structure of the central ion. Of the two hybrid functionals, it can be seen that $\langle \hat{S}^2 \rangle$ are slightly improved when using the BHLYP functional, which also gives slightly more accurate Ln-O and Ln-N bond lengths, particularly for the heavier lanthanides. This latter finding is in agreement with previous computational studies[16,79]. For these reasons, and due to the fact that hybrid-functionals with a high contribution of exact exchange partially suppress the effects self-interaction in heavy element complexes, we focus only on B3LYP- and BHLYP-derived electronic structures for the remainder of this contribution. In order to reduce the effects of spin contamination in the complexes of the Gd, Tb and Dy, the spin-constrained approach of Andrews *et al*.[80] was employed in subsequent single-point energy calculations of these systems.

Topological analysis of the electron density

To investigate any variation in bonding character in the complexes under consideration here as the lanthanide series was traversed, we employed the Quantum Theory of Atoms in Molecules (QTAIM). To improve on our description of the electronic structure at our optimised geometries, we performed single-point energy calculations using polarised triple-ζ quality basis sets and analysed the resultant electron density distributions.

QTAIM partitions a molecular system into a contiguous space-filling set of atomic volumes, each of which is bounded by a zero flux surface satisfying the condition $\nabla\rho(\mathbf{r}) \cdot n(\mathbf{r}) = 0$, where $\rho(\mathbf{r})$ is the magnitude of the electron density at **r** and $n(\mathbf{r})$ as a vector normal to the surface at **r**. If a minimum in

$\rho(\mathbf{r})$ between two nuclei coincides with the interatomic surface defined by the zero flux condition, then the two corresponding atoms are considered to be chemically bound, and this minimum in $\rho(\mathbf{r})$ is characterised as a bond critical point (BCP). The line of minimum $\rho(\mathbf{r})$ between two nuclei which passes through the BCP is characterised the bond path. The bond (and other) critical points, along with the bond paths, collectively comprise the molecular graph of the system (see Figure 3).

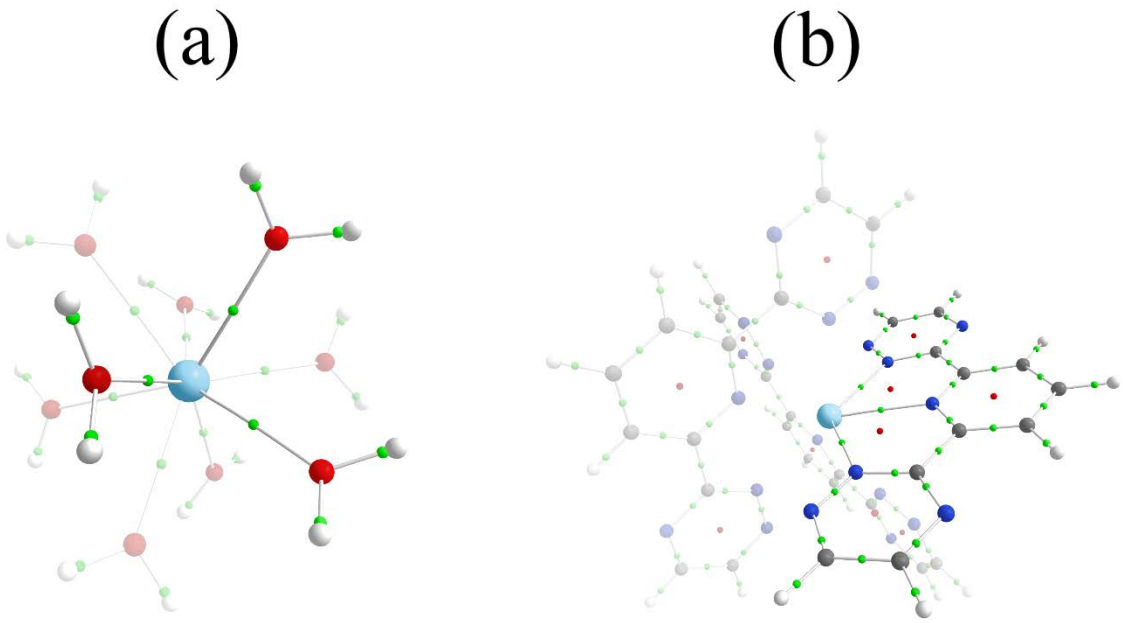

Figure 3. Representative molecular graphs of (a) $[Ln(H_2O)_9]^{3+}$and (b) $[Ln(BTP)_3]^{3+}$. Sky blue, red, blue, grey and white spheres represent Ln, O, N, C, and H atoms, respectively. Small green and red spheres represent bond critical points (BCPs) and ring critical points (RCPs), respectively. For clarity, selected Ln – N and inter-ligand bond paths have been removed from (b).

Typically, three properties of the electron density at the BCP are used to characterise a bonding interaction: the magnitude of the electron density ($\rho_{\mathbf{BCP}}$), which is large and positive (typically > 0.2 a.u.) for a covalent interaction, it's Laplacian ($\nabla^2\rho_{\mathbf{BCP}}$), which is negative for a covalent interaction, and the energy density at the BCP ($H_{\mathbf{BCP}}$), which is also negative for a covalent interaction. These three metrics can therefore be used to broadly characterise a bonding interaction as covalent or ionic,

but also allow for variations in covalent/ionic character to be identified. These metrics are summarised in Figure 4 (see Tables S5 and S6 of ESI for numerical values).

Focussing first on values averaged over the Ln series (See Tables S5 and S6 of ESI), the small value of $\bar{\rho}_{\mathbf{BCP}}$ and the positive value of its Laplacian are indicative of the expected ionic nature of the metal-ligand interactions in both the aquo and BTP complexes. Whilst $\bar{H}_{\mathbf{BCP}}$ is negative for both sets of complexes, its magnitude is so small that is more appropriately considered as being $\simeq 0$.

When considering variation of $\rho_{\mathbf{BCP}}$ across the Ln series, an increasing trend is seen as the series is traversed, although this increase is very weak. For the aquo complexes, BHLYP-derived maximum and minimum values lie 2.9% and 5.4% from the mean, respectively, and the mean absolute deviation (MAD) across the series is just 1.8% of the mean value. B3LYP-derived maximum and minimum values lie 2.7% and 4.8% from the mean, respectively, and the mean absolute deviation (MAD) across the series is just 1.6% of the mean value. For the BTP complexes, this variation is even less pronounced: BHLYP-derived maximum and minimum values lie only 1.4% and 3.1% from the mean, respectively, with the MAD across the series being just 1.0% of the mean value. B3LYP-derived maximum and minimum values lie 1.9% and 2.7% from the mean, respectively, with the MAD across the series just 1.2% of the mean value.

Similar behaviour is seen for $\nabla^2\rho_{\mathbf{BCP}}$, although the increase across the series is more pronounced. For the aquo complexes, BHLYP-derived maximum and minimum values lie 13.2% and 13.8% from the mean, respectively, and the MAD across the series is 6.8% of the mean value. B3LYP-derived maximum and minimum values lie 12.1% and 15.7% from the mean, respectively, and the MAD across the series is 7.1% of the mean value. For the BTP complexes, BHLYP-derived maximum and minimum values lie 11.3% and 15.0% from the mean, respectively, and the MAD across the series is 6.5% of the mean value. B3LYP-derived maximum and minimum values lie 11.8% and 14.4% from the mean, respectively, and the MAD across the series is 6.1% of the mean value.

There is no clear trend in H_{BCP} for either set of complexes, but BHLYP-derived MADs are again just 7.0% and 3.4% of mean values for the aquo and BTP complexes, respectively. Corresponding B3LYP-derived MADs are 9.1% and 6.3% of mean values. This supports our assertion that H_{BCP} should be considered as being effectively equal to 0 in these complexes.

Taken together, this data indicates only extremely weak variation in bonding character across the Ln series, as would be expected when bonding is dominated by ionic interactions. Whilst variation in $\nabla^2\rho_{BCP}$ is more pronounced than that in ρ_{BCP} itself, the former is defined as the sum of the principal curvatures of the electron density at the BCP. It is therefore unsurprising that it is more sensitive to small changes in electronic structure at this critical point.

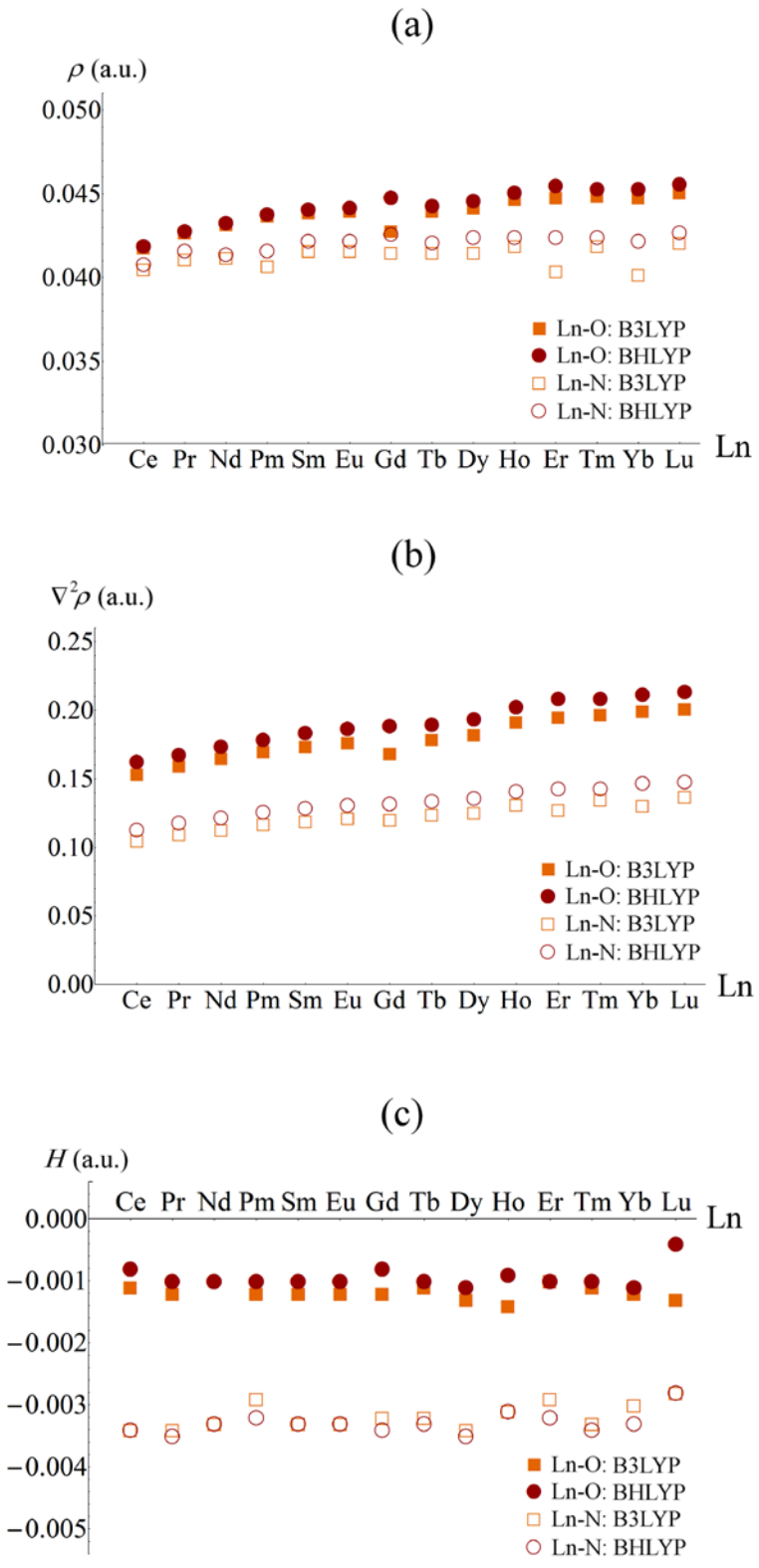

Figure 4. Topological analysis of BHLYP/def(2)-TZVP//BHLYP/def(2)-SVP and B3LYP/def(2)-TZVP//B3LYP/def(2)-SVP calculated electron densities at the Ln-O/Ln-N BCPs. (a) ρ = magnitude of electron density at BCP, (b) $\nabla^2\rho$ = Laplacian of ρ at BCP, (c) H = magnitude of energy density at BCP. Values are averaged over all BCPs.

Ln vs An bonding in $M(BTP)_3$ complexes

With regard to the separation of the minor actinides from lanthanides, much of the existing literature is focussed on the separation of the minor actinides americium and curium from europium. From a computational perspective however, it might be expected that Gd(III), being a formally $4f^7$ complex with a half-filled 4f-shell, might be more accurately simulated using the methodology employed here. Furthermore, the simulation of open-shell complexes is a challenge for density functional theory and so the ability to compare complexes with related electronic structures, i.e. $4f^7$ Gd(III) with $5f^7$ Cm(III) and $4f^6$ Eu(III) with $5f^6$ Am(III), might be expected to produce more reliable data. For this reason we here focus on the characterisation of bonding in BTP complexes of Am, Cm, Eu and Gd. To this end, we supplement the topological analysis discussed in the previous section with consideration also of integrated properties of the electron density, namely the atomic charge (a one-electron integrated property) and the localisation (λ) and delocalisation (δ) indices, both of which are formally two-electron properties. The delocalisation index can be considered as a measure of bond order in the absence of charge-transfer and, more generally, provides a quantitative measure of electron sharing between two atoms[81]. For this reason, it can be considered as a complementary measure of covalency to ρ_{BCP}. For states that can be described by a single electronic configuration, the delocalisation index can be defined in terms of the products of overlap integrals evaluated in neighbouring atomic basins, and therefore is large when orbital mixing is pronounced.

Tables 2 and 3 summarise the integrated QTAIM properties of the BTP complexes of Eu, Gd, Am and Cm. There is very little difference in atomic charges, with a slight excess of 0.02 a.u. on the Ln centres when compared to the An centres. We have previously argued[44,49,53] that localisation indices give more information with regard to bonding since electron density in an atomic basin can be partitioned into that which is localised in the basin and that which is delocalised between pairs of basins. The difference between the total electron density in the atomic basin and localisation index, $N(\mathrm{M}) - \lambda(\mathrm{M})$, therefore provides the number of electrons in the atomic basin that are delocalised, or

shared, with other basins. Table 2 reveals a significant increase of 18% for Am over Eu and 14% for Gd over Cm in this measure (irrespective of the functional employed), indicative of increased covalent interaction in the actinide systems.

Table 2. Integrated properties of BHLYP/def(2)-TZVP//BHLYP/def(2)-SVP and B3LYP/def(2)-TZVP//B3LYP/def(2)-SVP calculated electron densities of $M[(BTP)_3]^{3+}$ (M = Eu, Gd, Am, Cm). $N(\Omega)$ = Integrated electron density in atomic basin Ω, $q(\Omega)$ = total charge of basin Ω, $\lambda(\Omega)$ = localisation index of basin Ω. B3LYP-derived values given in parentheses. All values are in a.u.

M	$q(\mathrm{M})$	$N(\mathrm{M})-\lambda(\mathrm{M})$	$q(\mathrm{N_P})$	$\lambda(\mathrm{N_P})$	$q(\mathrm{N_T})$	$\lambda(\mathrm{N_T})$
Eu	+2.29 (+2.18)	1.04 (1.14)	-1.36 (-1.17)	6.66 (6.43)	-0.80 (-0.67)	6.04 (5.89)
Am	+2.27 (+2.17)	1.23 (1.34)	-1.36 (-1.16)	6.65 (6.41)	-0.81 (-0.67)	6.04 (5.88)
Gd	+2.29 (+2.19)	1.02 (1.11)	-1.36 (-1.17)	6.66 (6.44)	-0.80 (-0.68)	6.04 (5.89)
Cm	+2.27 (+2.17)	1.16 (1.27)	-1.35 (-1.17)	6.65 (6.42)	-0.80 (-0.67)	6.03 (5.88)

Table 3. Topological and integrated properties of BHLYP/def(2)-TZVP//BHLYP/def(2)-SVP and B3LYP/def(2)-TZVP//B3LYP/def(2)-SVP calculated electron densities of $M[(BTP)_3]^{3+}$ (M = Eu, Gd, Am, Cm). ρ_{BCP} = magnitude of electron density at BCP, $\delta(\Omega_1,\Omega_2)$ = delocalisation index between atomic basins Ω_1 and Ω_2. B3LYP-derived values given in parentheses. All values are in a.u.

M	$\delta(\mathrm{M},\mathrm{N_P})$	$\delta(\mathrm{M},\mathrm{N_T})$	$\rho_{\mathrm{BCP}}(\mathrm{M},\mathrm{N_P})$	$\rho_{\mathrm{BCP}}(\mathrm{M},\mathrm{N_T})$
Eu	0.201 (0.227)	0.204 (0.222)	0.0411 (0.0417)	0.0422 (0.0418)
Am	0.242 (0.265)	0.247 (0.262)	0.0425 (0.0433)	0.0442 (0.0448)
Gd	0.202 (0.229)	0.204 (0.219)	0.0414 (0.0420)	0.0426 (0.0414)
Cm	0.224 (0.245)	0.233 (0.251)	0.0423 (0.0426)	0.0445 (0.0442)

Atomic charges are also somewhat misleading when considering the coordinating nitrogens. Here we consider properties of the pyridine (N_P) and triazine (N_T) nitrogens separately. This is in contrast to Tables S5 and S6 which presents averaged values. Whilst N_P charges are ~ 0.5 a.u. larger than those of N_T, localisation indices are actually ~ 0.6 a.u. larger, suggesting that despite the excess charge on the N_P centre, less charge is being shared with coordinating species.

Turning our attention to measures of covalency, Table 3 shows that delocalisation indices are noticeably larger in the actinide complexes. This is most pronounced in the M – N_T interaction, commensurate with our analysis of localisation indices above. Averaged $\delta(M,N)$ values are 21% (17%) greater for Am in comparison to Eu and 13% (11%) greater for Cm in comparison to Gd when employing the BHLYP (B3LYP) functional. ρ_{BCP} values are also larger in the An complexes, particularly in the M – N_T bond, although this difference is less pronounced. Averaged values are 4% (5%) greater for Am in comparison to Eu and 3% (4%) greater for Cm in comparison to Gd when employing the BHLYP (B3LYP) functional. Combined, integrated and topological data indicate enhanced covalency in the Am and Cm complexes over that in the Eu and Gd analogues.

Averaging the M – N_T and M – N_P ρ_{BCP} values also allows for direct comparison with the mean Ln values presented in Tables S5 and S6. The averaged BHLYP-derived An value, 0.0437 a.u., is 4% larger than the mean Ln value of 0.0421 a.u. This apparently modest difference in fact corresponds to a ρ_{BCP} value that is approximately three standard deviations larger than the mean Ln value. B3LYP-derived data reveals a similar increase of 6%, corresponding to a ρ_{BCP} value approximately four standard deviations larger than the mean Ln value: An – N ρ_{BCP} values are therefore demonstrated to be markedly larger than the corresponding Ln – N values.

While analysis of B3LYP- and BHLYP-derived densities reveals similar differences between Eu/Gd and Am/Cm bonding, there is significant disparity when BLYP densities are considered, with ratios of An/Ln QTAIM properties notably larger than those obtained from B3LYP and BHLYP densities.

Comparison can be found in Table S7 of ESI, which indicates that caution should be used when employing pure GGA functionals to study bonding in these systems.

Relative stabilities of aquo and TP complexes

To investigate the potential stability of BTP complexes of An over Ln analogues, and hence the selectivity of BTP for the former, we considered the following exchange reaction:

$$[An(H_2O)_9]^{3+} + [Ln(BTP)_3]^{3+} \rightarrow [Ln(H_2O)_9]^{3+} + [An(BTP)_3]^{3+} \quad (1)$$

The SCF energy of reaction (1) was first evaluated for Ln = Eu, Gd and An = Am, Cm using BHLYP/def(2)-TZVP calculated energies obtained at BHLYP/def(2)-SVP optimised geometries (see Table 4). These simulations revealed the Eu ↔ Am and Gd ↔ Cm exchange reactions to be very weakly favourable for the actinides, i.e. a weak selectivity of BTP for Am over Eu and Cm over Gd. Whilst the Gd ↔ Am reaction was also found to be favourable, the Eu ↔ Cm reaction was not. As discussed above, it might be expected that the Eu ↔ Am and Gd ↔ Cm reactions would be more reliably modelled than the Eu ↔ Cm and Gd ↔ Am reactions, and the very similar reaction energies appear to bear this assumption out. B3LYP/def(2)-TZVP//B3LYP/def2-SVP calculated all reactions to be favourable for both Am and Cm, although it should be borne in mind that a spin-constrained simulation was required for $[Gd(BTP)_3]^3$.

To investigate basis set dependence on reaction energies, aquo and BTP complexes of Eu, Gd, Am and Cm were reoptimised using the BHLYP/def(2)-TZVP model chemistry (although vibrational frequency analysis could not be performed due to computational expense). These optimisations revealed only very slight variations in reaction energy of ≤ 0.01 eV that were, nevertheless, consistently in favour of the actinide complex. Such small variation in reaction energies justifies the

use of the BHLYP/def(2)-TZVP//BHLYP/def(2)-SVP and B3LYP/def(2)-TZVP//B3LYP/def(2)-SVP model chemistries.

Table 4. SCF energies of exchange reaction (1) for Ln = Eu, Gd and An = Am, Cm, calculated using the BHLYP/def(2)-TZVP//BHLYP/def2-SVP and B3LYP/def(2)-TZVP//B3LYP/def2-SVP model chemistry. Values in parentheses were obtained using the BHLYP/def2-TZVP model chemistry. *****$[Gd(BTP)_3]^{3+}$ single point energy obtained using the spin-constrained approach of Andrews *et al*.[80]

Reaction	E_r			
	eV		**kJ/mol**	
	BHLYP	**B3LYP**	**BHLYP**	**B3LYP**
Eu ↔ Am	-0.01 (-0.02)	-0.05	-0.96 (-1.93)	-4.82
Gd ↔ Cm	-0.02 (-0.02)	-0.12*	-1.93 (-1.93)	-11.58*
Eu ↔ Cm	+0.05 (+0.04)	-0.10	+4.82 (+3.86)	-9.65
Gd ↔ Am	-0.08 (-0.09)	-0.07*	-7.72 (-8.68)	-6.75*

The reaction energies required to give significant separation factors are not large: for example an energy difference of just 0.12 eV corresponds to a separation factor of 100, which in turn represents a 99% separation of species[82]. However, the prediction of such small relative energies presents a significant computational challenge using currently practicable methodologies. Whilst the reaction energies presented in Table 4, taken in the context of the bonding analysis performed here, are broadly supportive of very weak covalency-induced stabilisation of $[An(BTP)_3]^{3+}$, we calculated the same reaction energies for the entire Ln series in an attempt to gain a better understanding of the apparent stability of the An complexes. These reactions energies are summarised in Figure 5. Surprisingly, a strong trend across the series was found, with the exception of the Pm ↔ Am reaction, for which an anomalous value ~ 6 eV too large was obtained and could not be eliminated via spin-constrained calculations. While there is significant variation between adjacent data points, there is a broad increase in the relative stability of $[Ln(BTP)_3]^{3+}$ as atomic number increases. Whilst the An complexes are strongly stable in comparison to early Ln analogues, the energy difference is marginal for Eu and beyond, with BTP complexes of later lanthanides predicted to be stable relative to the Am

and Cm analogues. An explanation for this apparent stability may lie in the model used in this study. This model assumes an aquo complex in which the lanthanide ion is nine-coordinated. This is in accurate model up to Ln = Gd, where calculated coordination numbers are in agreement with experiment, but beyond this there is debate as to whether the coordination number drops to eight. EXAFS data[38] show a reduction in coordination number below nine (though not as low as eight) for Ln > Gd, and a recent *ab initio* molecular dynamics study of the hydration of Dy(III) and Ho(III) conclude that eight-coordinated complexes are energetically stable[83]. This implies that, for Ln > Gd the nine-coordinated models used here may not be representative of the most stable aquo complex, leading to an artificial *apparent* stabilisation of the BTP complex when the exchange reaction (1) is considered. From a computational perspective, the methodology employed here does not allow for an unbiased comparison between eight and nine-coordinated aquo complexes in the exchange reactions, and the inclusion of a continuum solvent, which results in significantly more accurate molecule structures, is incompatible with an '8+1' aquo model with one water in a second solvation shell.

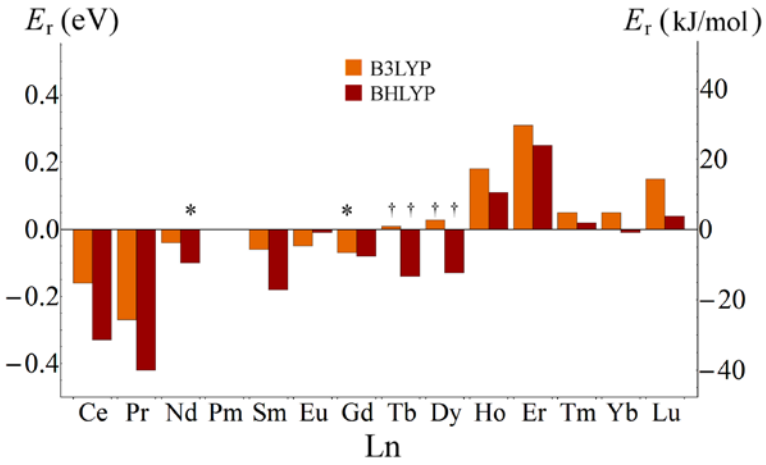

Figure 5. Energies of exchange reaction (1) for Ln = Ce-Lu and An = Am, calculated using the BHLYP/def(2)-TZVP//BHLYP/def(2)-SVP and B3LYP/def(2)-TZVP//B3LYP/def(2)-SVP model chemistries. *****$[Ln(BTP)_3]^{3+}$ single point energy obtained using the spin-constrained approach of Andrews *et al.*[80] **†**$[Ln(BTP)_3]^{3+}$ and $[Ln(H_2O)_9]^{3+}$ single point energies obtained using the spin-constrained approach. Reaction energies for An = Cm show an identical trend, and are uniformly shifted upwards by 0.06 eV at the BHLYP level and down by 0.05 eV at the B3LYP level. The anomalous reaction energy for Ln = Pm is omitted for clarity.

Integrated QTAIM properties of Ln and An aquo complexes

If the weak energetic favourability of the Eu ↔ Am and Gd ↔ Cm exchange reactions discussed above is due to covalent stabilisation of the An – N bond, then the difference in covalent character between the An – N and Ln – N bonds would be expected to be more pronounced than in the An – O and Ln – O bonds of the aquo complexes. In Table 5 we summarise the relevant topological and integrated properties of $M[(H_2O)_9]^{3+}$ (M = Eu, Gd, Am, Cm). When considering the number of non-localised electrons in the metal basin, $N(\mathrm{M}) - \lambda(\mathrm{M})$, there is increase of 11% for Am over Eu and 5% for Gd over Cm when employing the BHLYP level, significantly less than the differences of 18% and 14% found in the BTP complexes. When employing the B3LYP functional this difference is less marked: an increase of 13% for both Am over Eu and Gd over Cm. This behaviour is replicated in $\delta(\mathrm{M,O})$ values, which are 12% greater for Am in comparison to Eu and 7% greater for Cm in comparison to Gd when using the BHLYP functional. For comparison, averaged $\delta(\mathrm{M,N})$ values are 21% greater for Am in comparison to Eu and 13% greater for Cm in comparison to Gd. When employing the B3LYP functional, an increase of 13% is found for both Am over Eu and Gd over Cm, in comparison to increases of 17% and 11% in the BTP complexes.

Finally, BHLYP-derived ρ_{BCP} values are 3% greater for Am in comparison to Eu and actually slightly smaller for Cm in comparison to Gd. The mean An – O ρ_{BCP} value of 0.452 a.u. is 2% larger, and within one standard deviation of, the mean Ln – O value. In comparison, An – N ρ_{BCP} values are 4% larger, and three standard deviations from, the mean Ln – N value. B3LYP derived data reveals a similar relationship: ρ_{BCP} values are 3% greater for Am in comparison to Eu and 5% greater for Cm in comparison to Gd. The mean An – O ρ_{BCP} value of 0.452 a.u. is 3% larger, and approximately one standard deviation from, the mean Ln – O value. B3LYP-derived An – N ρ_{BCP} values are 6% larger, and four standard deviations from, the mean Ln – N value.

Table 5. Integrated properties of BHLYP/def(2)-TZVP//BHLYP/def(2)-SVP and B3LYP/def(2)-TZVP//B3LYP/def(2)-SVP calculated electron densities of $M[(H_2O)_9]^{3+}$ (M = Eu, Gd, Am, Cm). $N(\Omega)$ = Integrated electron density in atomic basin Ω, $q(\Omega)$ = total charge of basin Ω, $\lambda(\Omega)$ = localisation index of basin Ω. B3LYP-derived values given in parentheses. All values are in a.u.

M	$q(\mathrm{M})$	$N(\mathrm{M}) - \lambda(\mathrm{M})$	$q(\mathrm{O})$	$\lambda(\mathrm{O})$	$\delta(\mathrm{M},\mathrm{O})$	$\rho_{\mathrm{BCP}}(\mathrm{M},\mathrm{O})$
Eu	+2.44 (+2.38)	0.94 (1.00)	-1.24 (-1.20)	8.45 (8.38)	0.200 (0.214)	0.0443 (0.0440)
Am	+2.46 (+2.38)	1.04 (1.13)	-1.27 (-1.20)	8.49 (8.37)	0.223 (0.242)	0.0455 (0.0454)
Gd	+2.41 (+2.37)	0.96 (0.98)	-1.30 (-1.20)	8.51 (8.38)	0.203 (0.209)	0.0451 (0.0425)
Cm	+2.46 (+2.37)	1.01 (1.11)	-1.27 (-1.20)	8.50 (8.37)	0.218 (0.236)	0.0449 (0.0448)

Conclusions

Complexes of the lanthanides are routinely considered as being dominated by ionic metal ligand interactions, although rare exceptions exist in the literature. This ionic bonding character does not, however, preclude complex electronic structures that may be difficult to characterise using orbital-based analysis techniques. Actinide complexes are increasingly subjected to analysis via Bader's QTAIM approach which is able to characterise and quantify variation in bonding character. Lanthanide complexes have, however, never being systematically analysed using this methodology. If the QTAIM approach is to be broadly applicable across the f-elements, it must be ensured that it is consistent in its characterisation of the lanthanides, allowing for subtle differences in bonding character between complexes the lanthanides and actinides to be characterised and quantified.

In this contribution, we have performed QTAIM analysis on $Ln[(H_2O)_9]^{3+}$ and $[Ln(BTP)_3]^{3+}$ complexes, where Ln = Ce - Lu. Analysis was performed on DFT-optimised electron densities, using the BHLYP/def(2)-TZVP//BHLYP/def(2)-SVP and B3LYP/def(2)-TZVP//B3LYP/def(2)-SVP model chemistries. The BHLYP functional, in particular, has previously been demonstrated effective in

suppressing artefactual covalent bond character from complexes of late lanthanides by reducing the effects of self-interaction. This analysis revealed that QTAIM predicts that, for both sets of complexes, bonding across the lanthanide series is largely similar and ionic in character, as would be expected, demonstrating the applicability of the analytical method to these systems.

Whether the decision is made to recycle or dispose of spent nuclear fuel, efficient strategies require the separation of lanthanides and actinides. A great deal of progress has been made on chemical Ln/An separation via solvent extraction techniques and there is a belief that part of the success attributed to this approach is due to enhanced covalent interactions between selective ligands and An ions which leads to increased stability of An complexes over Ln analogues. Here we have shown evidence of weak selectivity of the BTP ligand for Am over Eu and Cm over Gd and demonstrated a commensurate increase in covalent bonding character for An BTP complexes over Ln analogues, greater than that found in corresponding aquo complexes, implying a small electronic contribution to the selectivity found experimentally. This finding may be of potential benefit to separation process design in future fuel cycles. Future work will focus on approaches that enhance this contribution as well as the development of model complexes to which higher-level theoretical methodologies can be applied.

Supporting Information Available: Structural parameters, reaction energies and topological data.

Acknowledgements

AK thanks the EPSRC for the award of a career acceleration fellowship (Grant EP/J002208/1). We thank the Nuclear Decommissioning Authority for financial support, the National Nuclear Laboratory for industrial supervision and acknowledge both the High End Computing facility at Lancaster University for access to HPC resources and the National Service for Computational Chemistry Software for access to the Slater HPC facility. We also thank Dr. Michael Patzschke and Mr. Yoshinobu Ebashi for helpful discussions and Mr. Oscar Marshall for technical support. All data

created during this research are openly available from the Lancaster University data archive at http://dx.doi.org/10.17635/lancaster/researchdata/70.

References

(1) Dam, H. H.; Reinhoudt, D. N.; Verboom, W. *Chem. Soc. Rev.* **2007**, *36*, 367–377.

(2) Kolarik, Z. *Chem. Rev.* **2008**, *108*, 4208–4252.

(3) Lewis, F.; Hudson, M.; Harwood, L. *Synlett* **2011**, *2011*, 2609–2632.

(4) Hudson, M. J.; Harwood, L. M.; Laventine, D. M.; Lewis, F. W. *Inorg. Chem.* **2013**, *52*, 3414–3428.

(5) Panak, P. J.; Geist, A. *Chem. Rev.* **2013**, *113*, 1199–1236.

(6) Kolarik, Z.; Müllich, U.; Gassner, F. *Solvent Extr. Ion Exch.* **1999**, *17*, 23–32.

(7) Kolarik, Z.; Müllich, U.; Gassner, F. *Solvent Extr. Ion Exch.* **1999**, *17*, 1155–1170.

(8) Steppert, M.; Walther, C.; Geist, A.; Fanghänel, T. *New J. Chem.* **2009**, *33*, 2437.

(9) Colette, S.; Amekraz, B.; Madic, C.; Berthon, L.; Cote, G.; Moulin, C. *Inorg. Chem.* **2002**, *41*, 7031–7041.

(10) Colette, S.; Amekraz, B.; Madic, C.; Berthon, L.; Cote, G.; Moulin, C. *Inorg. Chem.* **2004**, *43*, 6745–6751.

(11) Trumm, S.; Panak, P. J.; Geist, A.; Fanghänel, T. *Eur. J. Inorg. Chem.* **2010**, *2010*, 3022–3028.

(12) Trumm, S.; Lieser, G.; Foreman, M. R. S. J.; Panak, P. J.; Geist, A.; Fanghänel, T. *Dalton Trans.* **2010**, *39*, 923–929.

(13) Ruff, C. M.; Müllich, U.; Geist, A.; Panak, P. J. *Dalton Trans.* **2012**, *41*, 14594–14602.

(14) Beele, B. B.; Rüdiger, E.; Schwörer, F.; Müllich, U.; Geist, A.; Panak, P. J. *Dalton Trans.* **2013**, *42*, 12139–12147.

(15) Denecke, M. a.; Panak, P. J.; Burdet, F.; Weigl, M.; Geist, A.; Klenze, R.; Mazzanti, M.; Gompper, K. *Comptes Rendus Chim.* **2007**, *10*, 872–882.

(16) Denecke, M. A.; Panak, P. J.; Weigl, M.; Schimmelpfennig, B.; Geist, A. *Inorg. Chem.* **2005**, *44*, 8418–8425.

(17) Banik, N. L.; Denecke, M. A.; Geist, A.; Modolo, G.; Panak, P. J.; Rothe, J. *Inorg. Chem. Commun.* **2013**, *29*, 172–174.

(18) Banik, N. L.; Schimmelpfennig, B.; Marquardt, C. M.; Brendebach, B.; Geist, A.; Denecke, M. A. *Dalton Trans.* **2010**, *39*, 5117-5122.

(19) Berthet, J.-C.; Miquel, Y.; Iveson, P. B.; Nierlich, M.; Thuéry, P.; Madic, C.; Ephritikhine, M. *J. Chem. Soc. Dalt. Trans.* **2002**, *2*, 3265–3272.

(20) Drew, M. G. B.; Guillaneux, D.; Hudson, M. J.; Iveson, P. B.; Russell, M. L.; Madic, C. *Inorg. Chem. Commun.* **2001**, *4*, 12–15.

(21) Iveson, P. B.; Rivière, C.; Nierlich, M.; Thuéry, P.; Ephritikhine, M.; Guillaneux, D.; Madic, C. *Chem. Commun.* **2001**, 1512–1513.

(22) Hülsen, M.; Weigand, A.; Dolg, M. *Theor. Chem. Acc.* **2008**, *122*, 23–29.

(23) Moritz, A.; Cao, X.; Dolg, M. *Theor. Chem. Acc.* **2006**, *117*, 473–481.

(24) Trumm, M.; Schimmelpfennig, B.; Geist, A. **2015**, *60*, 847–851.

(25) Lan, J.-H.; Shi, W.-Q.; Yuan, L.-Y.; Zhao, Y.-L.; Li, J.; Chai, Z.-F. *Inorg. Chem.* **2011**, *50*, 9230–9237.

(26) Lan, J.-H.; Shi, W.-Q.; Yuan, L.-Y.; Feng, Y.-X.; Zhao, Y.-L.; Chai, Z.-F. *J. Phys. Chem. A* **2012**, *116*, 504–511.

(27) Guillaumont, D. *J. Phys. Chem. A* **2004**, *108*, 6893–6900.

(28) Lewis, F. W.; Harwood, L. M.; Hudson, M. J.; Drew, M. G. B.; Hubscher-Bruder, V.; Videva, V.; Arnaud-Neu, F.; Stamberg, K.; Vyas, S. *Inorg. Chem.* **2013**, *52*, 4993–5005.

(29) Lan, J.-H.; Shi, W.-Q.; Yuan, L.-Y.; Li, J.; Zhao, Y.-L.; Chai, Z.-F. *Coord. Chem. Rev.* **2012**,

256, 1406–1417.

(30) de Sahb, C.; Watson, L. a; Nadas, J.; Hay, B. P. *Inorg. Chem.* **2013**, *52*, 10632–10642.

(31) Yang, Y.; Hu, S.; Fang, Y.; Wei, H.; Hu, S.; Wang, D.; Yang, L.; Zhang, H.; Luo, S. *Polyhedron* **2015**, *95*, 86–90.

(32) Zaiter, A.; Amine, B.; Bouzidi, Y.; Belkhiri, L.; Boucekkine, A.; Ephritikhine, M. *Inorg. Chem.* **2014**, *53*, 4687–4697.

(33) Yang, Y.; Liu, J.; Yang, L.; Li, K.; Zhang, H.; Luo, S.; Rao, L. *Dalt. Trans.* **2015**, 44, 8959–8970.

(34) Bryantsev, V. S.; Hay, B. P. *Dalt. Trans.* **2015**, 44, 7935–7942.

(35) Marie, C.; Miguirditchian, M.; Guillaumont, D.; Tosseng, A.; Berthon, C.; Guilbaud, P.; Duvail, M.; Bisson, J.; Guillaneux, D.; Pipelier, M.; Dubreuil, D. *Inorg. Chem.* **2011**, *50*, 6557–6566.

(36) Petit, L.; Adamo, C.; Maldivi, P. *Inorg. Chem.* **2006**, *45*, 8517–8522.

(37) Trumm, M.; Schimmelpfennig, B. **2016**, *114*, 876–883.

(38) D'Angelo, P.; Spezia, R. *Chem. Eur. J.* **2012**, *18*, 11162–11178.

(39) Bader, R. F. W. *Atoms in Molecules: A Quantum Theory*; Oxford University Press: Oxford, 1990.

(40) Tassell, M. J.; Kaltsoyannis, N. *Dalt. Trans.* **2010**, *39*, 6576–6588.

(41) Kirker, I.; Kaltsoyannis, N. *Dalton Trans.* **2011**, *40*, 124–131.

(42) Kaltsoyannis, N. *Inorg. Chem.* **2013**, *52*, 3407–3413.

(43) Vallet, V.; Wahlgren, U.; Grenthe, I. *J. Phys. Chem. A* **2012**, *116*, 12373–12380.

(44) Kerridge, A. *RSC Adv.* **2014**, *4*, 12078–12086.

(45) Foroutan-Nejad, C.; Vícha, J.; Marek, R.; Patzschke, M.; Straka, M. *Phys. Chem. Chem. Phys.*

2015, *17* (37), 24182–24192.

(46) Clark, A. E.; Sonnenberg, J. L.; Hay, P. J.; Martin, R. L. *J. Chem. Phys.* **2004**, *121*, 2563–2570.

(47) Huang, Q.-R.; Kingham, J. R.; Kaltsoyannis, N. *Dalt. Trans.* **2015**, *44*, 2554–2566.

(48) Woodall, S. D.; Swinburne, A. N.; Kerridge, A.; Pietro, P. Di; Adam, C.; Kaden, P.; Natrajan, L. S. *Chem. Commun.* **2015**, *51*, 5402–5405.

(49) Di Pietro, P.; Kerridge, A. *Inorg. Chem.* **2016**, *55*, 573–583.

(50) Di Pietro, P.; Kerridge, A. *Phys. Chem. Chem. Phys.* **2016**, *18*, 16830–16839.

(51) Arnold, P. L.; Turner, Z. R.; Kaltsoyannis, N.; Pelekanaki, P.; Bellabarba, R. M.; Tooze, R. P. *Chem. - A Eur. J.* **2010**, *16*, 9623–9629.

(52) Kerridge, A. *Dalton Trans.* **2013**, *42*, 16428–16436.

(53) Beekmeyer, R.; Kerridge, A. *Inorganics* **2015**, *3*, 482–499.

(54) Gregson, M.; Lu, E.; Tuna, F.; McInnes, E. J. L.; Hennig, C.; Scheinost, A. C.; McMaster, J.; Lewis, W.; Blake, A. J.; Kerridge, A.; Liddle, S. *Chem. Sci.* **2016**, *7*, 3286–3297.

(55) Herve, A.; Bouzidi, Y.; Berthet, J.; Belkhiri, L.; Thuery, P.; Boucekkine, A.; Ephritikhine, M. *Inorg. Chem.* **2014**, *53*, 6995.

(56) Wu, H.; Wu, Q.-Y.; Wang, C.-Z.; Lan, J.-H.; Liu, Z.-R.; Chai, Z.-F.; Shi, W.-Q. *Dalt. Trans.* **2015**, *44*, 16737–16745.

(57) Löble, M. W.; Keith, J. M.; Altman, A. B.; Stieber, S. C. E.; Batista, E. R.; Boland, K. S.; Conradson, S. D.; Clark, D. L.; Lezama Pacheco, J.; Kozimor, S. a.; Martin, R. L.; Minasian, S. G.; Olson, A. C.; Scott, B. L.; Shuh, D. K.; Tyliszczak, T.; Wilkerson, M. P.; Zehnder, R. a. *J. Am. Chem. Soc.* **2015**, *137*, 2506–2523.

(58) Krinsky, J. L.; Minasian, S. G.; Arnold, J. *Inorg. Chem.* **2011**, *50*, 345–357.

(59) Altman, A. B.; Pacold, J. I.; Wang, J.; Lukens, W. W.; Minasian, S. G. *Dalt. Trans.* **2016**.

(60) Ahlrichs, R.; Bär, M.; Häser, M.; Horn, H.; Kölmel, C. *Chem. Phys. Lett.* **1989**, *162*, 165–169.

(61) Becke, A. D. *Phys. Rev. A* **1988**, *38*, 3098–3100.

(62) Lee, C.; Yang, W.; Parr, R. G. *Phys. Rev. B* **1988**, *37*, 785–789.

(63) Becke, A. D. *J. Chem. Phys.* **1993**, *98*, 5648.

(64) Stephens, P.; Devlin, F.; Chabalowski, C.; Frisch, M. *J. Phys. Chem.* **1994**, *98*, 11623–11627.

(65) Becke, A. D. *J. Chem. Phys.* **1993**, *98*, 1372–1377.

(66) Weigend, F.; Ahlrichs, R. *Phys. Chem. Chem. Phys.* **2005**, *7*, 3297–3305.

(67) Dolg, M.; Stoll, H.; Preuss, H. *J. Chem. Phys.* **1989**, *90*, 1730–1734.

(68) Cao, X.; Dolg, M. *J. Chem. Phys.* **2001**, *115*, 7348.

(69) Küchle, W.; Dolg, M.; Stoll, H.; Preuss, H. *J. Chem. Phys.* **1994**, *100*, 7535.

(70) Klamt, A.; Schüürmann, G. *Perkins Trans.* **1993**, *2*, 799–805.

(71) Pantazis, D. a.; Neese, F. *J. Chem. Theory Comput.* **2009**, *5*, 2229–2238.

(72) Pantazis, D. a.; Neese, F. *J. Chem. Theory Comput.* **2011**, *7*, 677–684.

(73) Douglas, M.; Kroll, N. *Ann. Phys. (N. Y).* **1974**, *155*, 89–155.

(74) Hess, B. *Phys. Rev. A* **1986**, *33*, 3742–3748.

(75) Keith, T. A. *AIMAll (Version 14.11.23), TK Gristmill Software, Overl. Park KS, USA* **2014**.

(76) Lu, T.; Chen, F. *J. Comput. Chem.* **2012**, *33*, 580–592.

(77) D'Angelo, P.; Zitolo, A.; Migliorati, V.; Chillemi, G.; Duvail, M.; Vitorge, P.; Abadie, S.; Spezia, R. *Inorg. Chem.* **2011**, *50*, 4572–4579.

(78) Ciupka, J.; Cao-Dolg, X.; Wiebke, J.; Dolg, M. *Phys. Chem. Chem. Phys.* **2010**, *12*, 13215–13223.

(79) Dolg, M.; Cao, X.; Ciupka, J. *J. Electron Spectros. Relat. Phenomena* **2014**, *194*, 8–13.

(80) Andrews, J. S.; Jayatilaka, D.; Bone, R. G. A.; Handy, N. C.; Amos, R. D. *Chem. Phys. Lett.* **1991**, *183*, 423–431.

(81) Fradera, X.; Austen, M. A.; Bader, R. F. W. *J. Phys. Chem. A* **1999**, *103*, 304–314.

(82) Nash, K. L. In *Metal-Ion Separation and Preconcentration*; Bond, A. H., Dietz, M. L., Rogers, R. D., Eds.; ACS Publications, 1999; pp 52–78.

(83) Tirler, A. O.; Passler, P. P.; Rode, B. M. *Chem. Phys. Lett.* **2015**, *625*, 120–126.

For Table of Contents Only

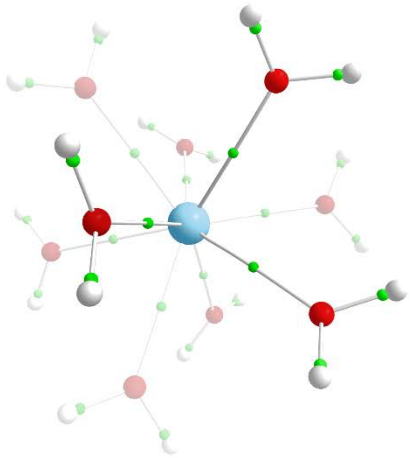

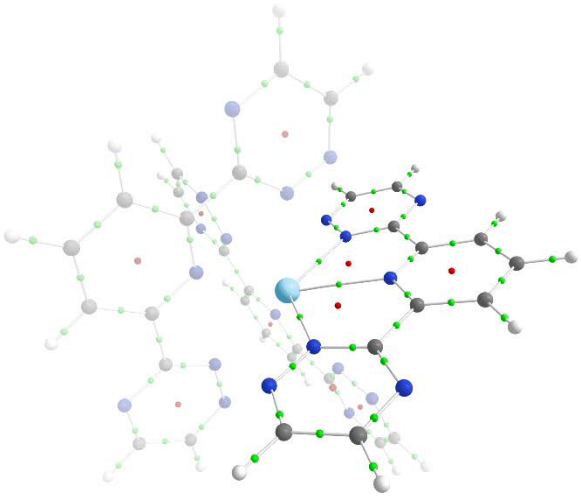

The electronic structures of $Ln[(H_2O)_9]^{3+}$ and $[Ln(BTP)_3]^{3+}$, (Ln = Ce – Lu) were simulated using Density Functional Theory (DFT) and analysed using the Quantum Theory of Atoms in Molecules (QTAIM). Comparisons were made to Americium and Curium analogues and it was found that covalency, according to QTAIM metrics, was enhanced in the latter. Exchange reaction energies were evaluated and supported weak selectivity of BTP for Am over Eu and Cm over Gd, implying a weak covalent stabilisation of the An – N bond.